

Direct experimental investigations of acoustic modes guided by a solid–solid interface using optical interferometry

Ch. Matteï,^{a)} X. Jia, and G. Quentin

Groupe de Physique des Solides, Université Paris 7, Unité associée au CNRS No. 17, tour 23,
2 place Jussieu, 75251 Paris Cedex 05, France

(Received 16 July 1996; revised 10 February 1997; accepted 11 February 1997)

This paper presents direct field measurements of acoustic modes guided by the interface between two transparent solids. The measurement technique is based on the acousto-optical interaction inside the solid between the acoustic field and the probe laser beam of an interferometer. The main advantage of the method is its ability to measure acoustic strain fields in areas of difficult access with the classic detection methods. Moreover, it gives complete information about the dilatation strain field inside the solid, e.g., amplitude and phase. The propagation of a real velocity mode (Stoneley wave) is first illustrated. Then the situation of complex velocity modes is investigated for a Plexiglas–fused quartz slip interface. This material combination supports two possible interface modes theoretically. These modes are simultaneously observed and the differences between their behavior are measured. © 1997 Acoustical Society of America. [S0001-4966(97)02006-7]

PACS numbers: 43.35.Sx, 43.35.Yb [HEB]

INTRODUCTION

Characterization of elastic properties of interfaces between solid media is a subject of fundamental interest in such fields as nondestructive testing¹ or geophysics.² Acoustic bulk waves, e.g., longitudinal or transverse waves, are sensitive to discontinuities that are characteristic of bond failures. Several methods^{3,4} have been developed in order to obtain information on interface qualities from transmission or reflection measurements of these acoustic bulk waves but these methods are hardly sensitive to fine details of interface properties. On the other hand, acoustic guided modes are confined in the interface region^{5,6} and their propagation properties are much more influenced by interface characteristics.⁷ Even so, only limited results of direct measurements of these guided waves have been obtained because of the difficulties associated to the interface access. As a matter of fact, most of these experimental works are phase velocity measurements using classic piezoelectric transducers. Lee and Corbly⁸ presented measurements of Stoneley waves and attenuated interface waves velocities in the aim of interface inspection.

An alternative to the classic piezoelectric transducer methods is the detection of interface waves by optical means. Claus and Palmer⁹ showed that optical detection methods could give more information than classical measurements; they detected the normal displacement of the interface and measured the Stoneley wavelength at a nickel–Pyrex interface.

Recent developments in optical interferometers dedicated to ultrasonic measurements made possible new types of measurements. Recently, Jia *et al.*¹¹ described a method based on the acousto-optic interaction which permits a local

measurement of the dilatation induced by a guided acoustic wave propagating inside a transparent solid. The main advantage of the method is its ability to measure acoustic strain fields in areas uneasy to probe with the classic detection methods. Moreover, it gives complete information on the dilatation strain field inside the solid, e.g., amplitude and phase.

In the context of interface waves studies, direct measurement of the acoustic field close to the interface is of primary interest. Measuring directly the inhomogeneity of the dilatation strain field gives a straightforward determination of the interface wave nature and it is the aim of this paper to present direct measurements of different kinds of interface waves using the interferometric detection method. Specifically, the simultaneous propagation of two leaky interface waves is presented. To our knowledge, this situation, which was predicted by Pilant¹² in a study of the complex roots of the solid–solid interface characteristic equation, has never been experimentally observed.

In the first part of the paper, principles of the interferometric detection method are presented and the experimental setup is shown. In the second part the classical characteristic equation roots problem for an interface between two solids is briefly presented and the nature of different interface modes is illustrated. The third part contains experimental results obtained with the interferometric detection method. First, direct measurements of the “Stoneley” wave (i.e., an interface wave propagating without loss along the interface) are shown for two different boundary conditions and two combinations of materials. Then the case of the simultaneous propagation of two leaky interface waves is presented. Velocities, attenuation, and field inhomogeneity are measured for both of them. The characteristics of these two interface modes are compared with the theoretical predictions and the physical difference between these two modes is discussed.

^{a)}Present address: Welding Engineering Institute, Ohio State University, 190 W. 19th Avenue, Columbus, OH 43210.

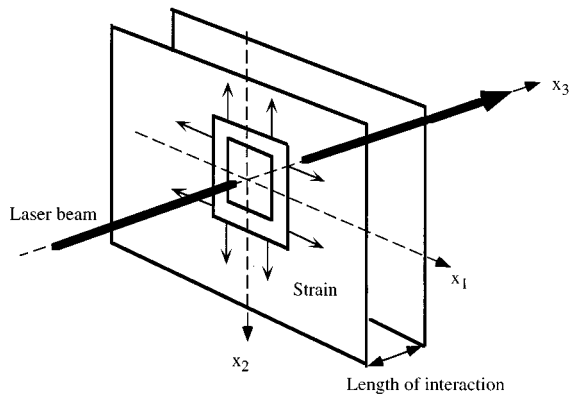


FIG. 1. Geometry of the acousto-optical interaction used for the interferometric detection method.

I. OPTICAL DETECTION TECHNIQUE AND EXPERIMENTAL SETUP

The optical detection technique used to investigate interface waves is based on an interferometric measurement of the dilatation induced by an acoustic guided wave propagating inside transparent materials. Like most of the acousto-optical detection techniques, this measurement is limited to two-dimensional (2-D) acoustic field probing. This technique has been applied first to Rayleigh wave detection¹³ and to Lamb wave-field measurements inside transparent plates.¹¹ This section presents the principles of the detection method. A more complete analysis of the acousto-optical interaction involved in this technique has been presented in a previous paper.¹¹

When an acoustic wave propagates inside an isotropic transparent solid of optical index $n = \epsilon^2$, the solid becomes optically birefringent and a light beam crossing the acoustic wave orthogonally undergoes a phase shift. Let us consider a guided acoustic wave with its displacement components in the sagittal plan (O, χ_1, χ_2) , defined by its strain tensor S_{kl} as shown in Fig. 1. As a result of the acoustic perturbation, the solid medium becomes optically anisotropic. The corresponding changes for the dielectric tensor are^{14,15}

$$\Delta \epsilon_{ij} = \Delta(n^2)_{ij} = -\epsilon^2 p_{ijkl} S_{kl}, \quad (1)$$

where n is the optical index of the medium and p_{ijkl} are the photoelastic constants of the material. The effect of the optical index variations on a beam crossing the solid medium are twofold: the transmitted light exhibits polarization and phase changes.¹⁵ For a laser beam much narrower than the acoustic wavelength, crossing an acoustic beam orthogonally propagating in the x_3 direction, the variation of the optical index induces a phase shift $\delta\varphi$:¹¹

$$\delta\varphi = -n^3 \frac{\omega l}{2c} (p_{11} + p_{22})(S_1 + S_2), \quad (2)$$

where ω is the optical frequency, c the velocity of the light in the material, and l the lateral dimension (measured along χ_3) of the acoustic beam and where the photoelastic constants and strains are written using the usual reduced matrix notation.

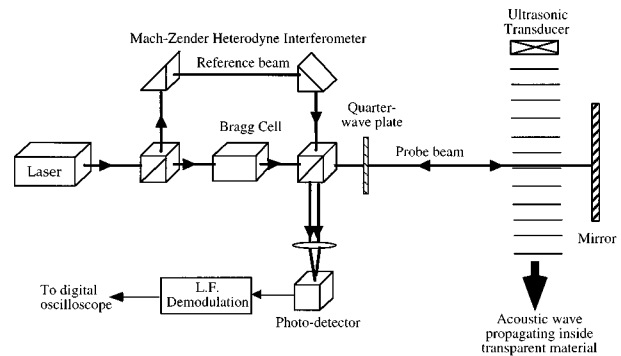


FIG. 2. Schematic diagram of the dilatation strain measurement with a Mach-Zender interferometer.

This optical phase shift can be measured using a Mach-Zender interferometer.¹⁶ The light coming from a He-Ne laser is divided into two beams (Fig. 2). The reference beam goes directly to a photodiode, whereas the probe beam, shifted in frequency by a Bragg cell ($f_b = 70$ MHz), crosses the acoustic beam back and forth and interferes with the reference beam on a photodiode. The phase shift $\delta\varphi$ is demodulated from the photocurrent by a broadband electronic processing used in acoustic displacement measurements.¹⁶ Finally, the signal at the output of the interferometer is a time signal, proportional to the acoustic dilatation strain, containing both amplitude and phase information. A sensitivity of 1 mV for a 10^{-7} strain is obtained inside fused quartz.¹¹

The quantity measured ($S_1 + S_2$) is analog to the relative dilatation $\Delta V/V$ inside the solid and will be noted underbar $\underline{\Delta}$. It can be expressed for harmonic acoustic waves as

$$\underline{\Delta} = (S_1 + S_2) = \text{div } \mathbf{u} = k^2 \phi, \quad (3)$$

where \mathbf{u} is the particle displacement vector, k the wave number, and ϕ the longitudinal potential.

The experimental setup is shown in Fig. 3. The samples are placed between the interferometer and a steady mirror. The laser beam orthogonally crosses back and forth the transparent materials to the acoustic beam and the optical phase shift induced by the optical index variations is detected by the interferometer. The corresponding electrical signal is

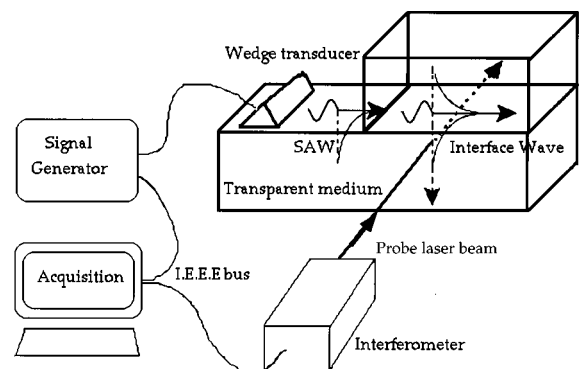


FIG. 3. Experimental setup used to generate and detect interface waves: The interface wave is generated by the conversion of a Rayleigh wave. The laser beam coming from the interferometer is crossing perpendicularly the transparent material.

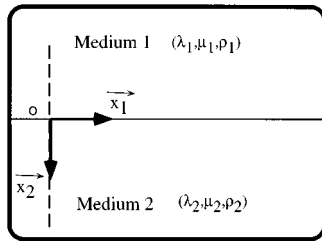


FIG. 4. Coordinate system for interface waves propagation.

collected at the output of the interferometer and sampled on a digital oscilloscope. Signal processing and representation is done on the sampled signal. By moving the sample in front of the interferometer, scans in the x_1 or x_2 direction can be done allowing velocity and attenuation measurements in the propagation direction as well as amplitude measurement in the direction normal to the interface.

II. INTERFACE WAVE PROPAGATION

In this section, we present briefly the solid–solid interface problem. The Cartesian system used in this description is shown in Fig. 4. The subscript 1 is dedicated to the upper medium and subscript 2 to the lower medium. The materials are defined by their Lamé constants and densities, λ_1, μ_1, ρ_1 and λ_2, μ_2, ρ_2 , respectively. In this system, the solutions of the equation of linear elasticity in each material can be written in terms of the longitudinal Φ and shear Ψ potentials in each medium,

$$\begin{aligned}\Phi_1 &= A_1 \exp(ik_z^1 z) \exp(i(k_x x - \omega t)), \\ \Psi_1 &= B_1 \exp(ik_z^1 z) \exp(i(k_x x - \omega t)), \\ \Phi_2 &= A_2 \exp(-ik_z^2 z) \exp(i(k_x x - \omega t)), \\ \Psi_2 &= B_2 \exp(-ik_z^2 z) \exp(i(k_x x - \omega t)),\end{aligned}\quad (4)$$

where $k_z^i = \sqrt{k_i^2 - k_x^2}$ and $k_z^i = \sqrt{k_i^2 - k_x^2}$ with $i=1,2$, and where k_x is the wave vector of the guided wave along the interface, and k_i, k_{t_i} are the longitudinal and shear wave number in the medium (i).

Two different sets of boundary conditions corresponding to experimental situations are chosen. The first ones are the slip boundary conditions, i.e., continuity of normal displacement, continuity of normal strain, and cancellation of transverse stress:

$$\begin{aligned}u_2(x_2=0^+) &= u_2(x_2=0^-), \\ T_{22}(x_2=0^+) &= T_{22}(x_2=0^-), \\ T_{12}(x_2=0^+) &= 0, \quad T_{12}(x_2=0^-) = 0.\end{aligned}\quad (5)$$

The second set describes the classic ‘‘bonded’’ conditions, i.e., continuity of both displacements and stresses:

$$\begin{aligned}u_1(x_2=0^+) &= u_1(x_2=0^-), \\ u_2(x_2=0^+) &= u_2(x_2=0^-), \\ T_{22}(x_2=0^+) &= T_{22}(x_2=0^-), \\ T_{12}(x_2=0^+) &= T_{12}(x_2=0^-).\end{aligned}\quad (6)$$

In each case, writing the four boundary conditions as a function of the potentials leads to a system of four linear equations with nontrivial solutions when its determinant is equal to zero.

The existence domain of a lossless interface mode (i.e., a real root, k_x , of the characteristic equations corresponding to the so-called Stoneley wave) has been studied by several authors. Scholte⁶ first showed that only a narrow range of material combinations support such interface waves in the case of bonded boundary conditions. Murty⁷ showed that this range was larger in the case of slip boundary conditions.

When the characteristic equation admits only complex values of k_x as solutions, Pilant¹² showed that, depending on the materials combination, two roots corresponding to leaky interface waves, i.e., roots with small imaginary parts, exist. He showed numerically that when the shear modulus of one of the material tends to zero (fluid–solid interface), one of these solutions approaches asymptotically the generalized Rayleigh wave. Under the same conditions, the other solution approaches the Scholte–Stoneley wave. By extension, he called the first mode the Rayleigh wave, and the second the Interface wave. Moreover, Pilant studied the existence domain for these two interface waves in function of the materials elastic constant in the case of bonded boundary conditions and found a range of material where both the Interface and Rayleigh waves can propagate. To our knowledge, the simultaneous propagation of these two modes has never been experimentally confirmed.

These three interface waves, Stoneley wave, Rayleigh wave, and Interface wave, have different field inhomogeneities which can be determined from the calculation of the potentials or the displacement fields in each material. The description of these interface modes in terms of a combination of inhomogeneous waves is also another way to determine these mode’s inhomogeneities.¹⁷ However, these two methods show the physical differences between these interface modes. As an example, the variation of the potentials in the direction perpendicular to the interface in each material is illustrated in Fig. 5 for the three interface waves. For the Stoneley wave, maximum amplitude for each potential is located near the interface. The two other modes are different in nature because at least one potential increases with increasing distance to the interface, i.e., part of the energy reradiates in one medium. Moreover, the radiation mechanism is not the same for these two modes. In the case of the Rayleigh wave, both longitudinal and shear potential amplitudes increase with the distance to the interface in one medium, whereas for the Interface mode the longitudinal potential is confined at the interface.

In practice, one of the difficulties when dealing with interface wave measurements is to clearly identify the measured interface modes among the 16 roots of the characteristic equation. Comparison between the measured and calcu-

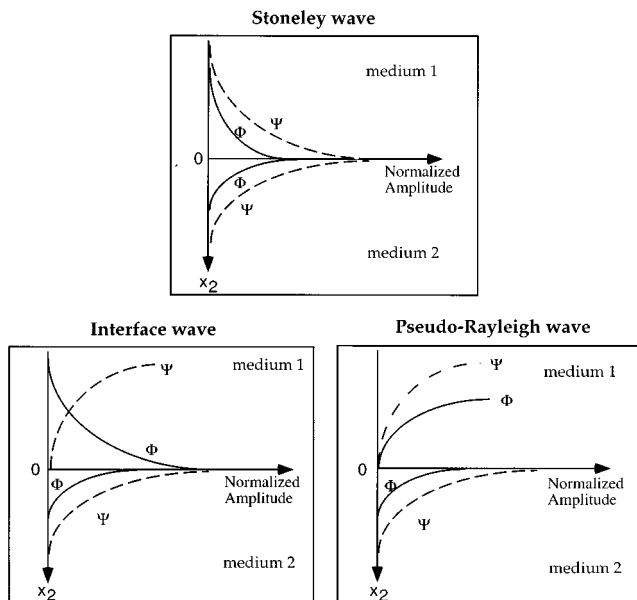


FIG. 5. Variation of the longitudinal (Φ) and shear (Ψ) potentials with the distance to the interface for the three interface waves involved: The Stoneley wave, the Interface wave, and the pseudo-Rayleigh wave (after Pilant).

lated velocities is the only way to achieve this identification with the classic piezoelectric detection techniques. The main feature of the interferometric detection method is its ability to measure the dilatation strain field, related to the longitudinal potential, in the materials as long as they are transparent. It gives the opportunity to measure in a simple way the field inhomogeneities of these interface modes. This information can be helpful in order to identify and characterize each mode as illustrated in the following section.

III. DIRECT MEASUREMENT OF INTERFACE WAVES

This section presents the experimental results obtained with the interferometric detection method. Three different combinations of materials are selected. In order to detect the Stoneley wave, the tungsten–fused quartz (bonded and slip boundary conditions) and the fused quartz–fused quartz (slip boundary conditions) combinations were selected. The case of leaky interface waves is investigated for the fused quartz–Plexiglas slip interface. The acoustical parameters of the three materials involved in these combinations are given in Table I.

The slip contact was achieved by setting a thin layer of water in between the optically polished materials. The thickness of the layer, estimated to 1–2 μm for water is far

TABLE I. Elastic characteristics of the different materials used in the experiments.

	Longitudinal velocity (m/s)	Transverse velocity (m/s)	Density kg/m^3
Fused quartz	5960	3760	2200
Tungsten	5220	2890	19 300
Plexiglas	2680	1100	1800

smaller than all the acoustic wavelengths. In the case of bonded contact, a film of glue (with a thickness estimated to 10 μm) is set in between the materials. The interface waves were generated using the conversion of a surface wave (Rayleigh wave) at the solid–solid interface. The Rayleigh wave is generated using the classic wedge technique, as shown in Fig. 2. Broadband pulses with a 1 MHz central frequency are used to generate the surface wave.

A. Direct Stoneley wave measurement

The characteristics of the detection technique are first illustrated in the case of a tungsten–fused quartz interface which supports a Stoneley wave for both bonded and slip boundary conditions. Because tungsten is a nontransparent material, the strain field measurements are only possible on one side of the interface, i.e., inside fused quartz. Figure 6 shows two records of the Stoneley wave taken at two different depths from the interface in the case of a bonded and a slip interface. The dilatation strain field confinement inside fused quartz is clearly seen in both cases.

By scanning the field in the direction parallel to the interface, velocity and attenuation measurements can be achieved. The measured velocities are $2.73 \times 10^3 (\pm 30)$ m/s for the slip interface and $2.86 \times 10^3 (\pm 30)$ m/s in the case of the bonded interface, in good agreement with the theoretical ones, respectively, 2.78×10^3 m/s and 2.89×10^3 m/s. In order to make sure that no attenuation occurs during the propagation, the spectra of two pulses are displayed on the same graph (Fig. 7). No evidence of attenuation is seen in both cases.

In order to scan the dilatation strain field on each side of the interface, a Stoneley wave is generated along a fused quartz–fused quartz slip interface. Figure 8 shows four time signals corresponding to a scan in the direction perpendicular to the interface. Only one mode is observed and this mode is clearly confined at the interface. The dilatation field presents a π phase shift on each side of the interface due to the flexural characteristics of the boundary motion. A scan in the direction parallel to the interface shows that the pulse propagates without measurable attenuation along a distance of 10 cm. By measuring the time of flight, a velocity of $3.34 \times 10^3 (\pm 30)$ m s⁻¹ is observed, close to the theoretical velocity of the Stoneley wave (3.36×10^3 m/s).

To measure quantitatively the decays in the x_2 direction of this mode, a method based on the Fourier spectral analysis of two records corresponding to two different depths is performed. In the case of an inhomogeneous plane wave, the Fourier transform of a dilatation strain pulse can be written without loss of generality

$$\Delta(x_1, x_2, k) = A(k)f(x_1)\exp(-\beta k x_2). \quad (7)$$

The term $A(k)$ is characteristic to the generation of the pulse and $f(x_1)$ to the propagation. Figure 9(a) shows two spectra of time signals corresponding to two measurements of the same pulse measured at constant x_1 but for two different x_2 in the medium 1. The ratio of these two spectra is

$$\exp(-\beta k(x_2' - x_2)), \quad (8)$$

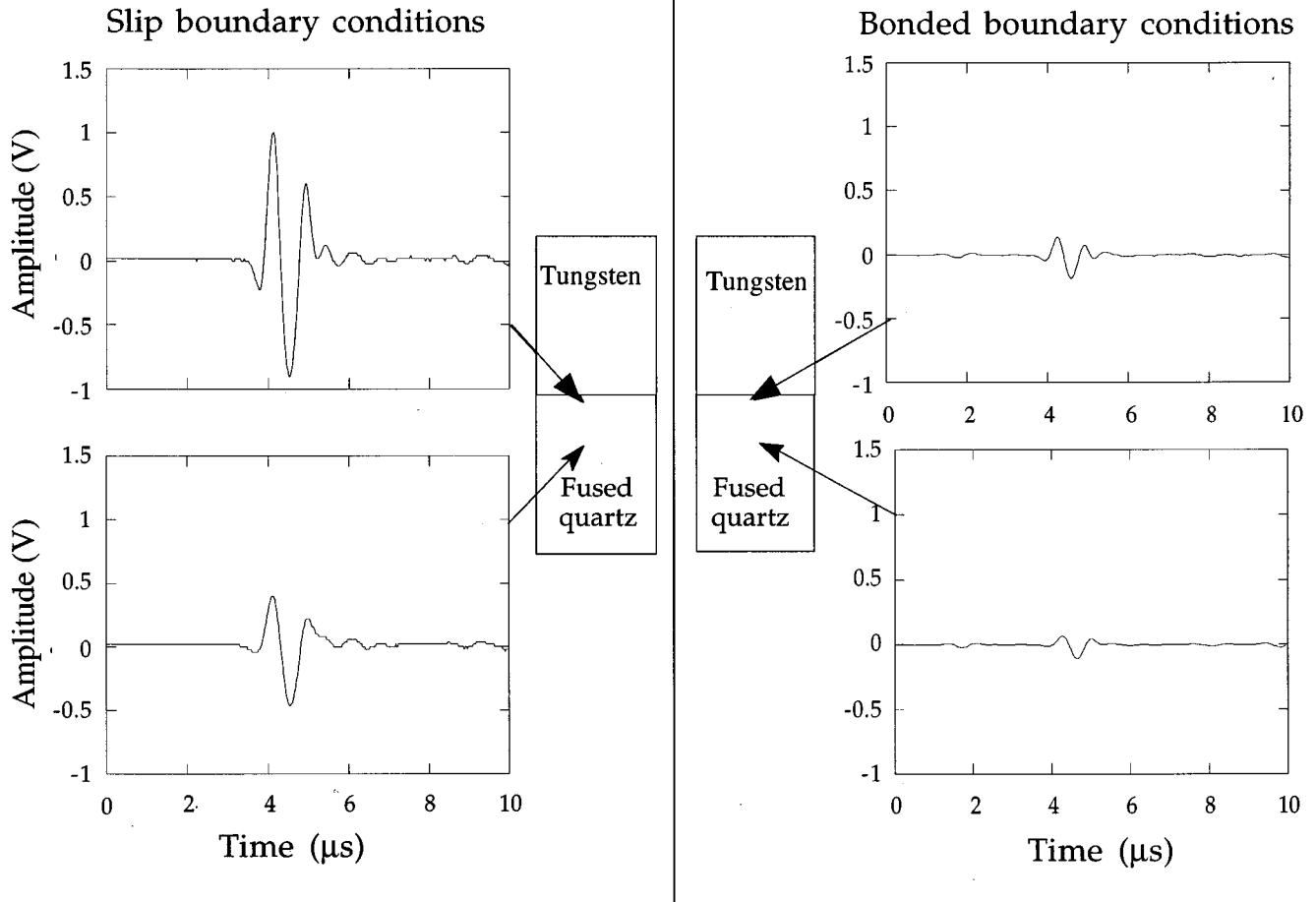


FIG. 6. Time signals corresponding to a scan in the z direction inside fused quartz for the tungsten–fused quartz for the bonded interface and the slip interface cases.

where x_2' and x_2 are the two absolute positions of the records. The same procedure can be applied in the other medium.

Figure 9(b) shows a plot of the measured decay on one side of the interface represented as a function of the fre-

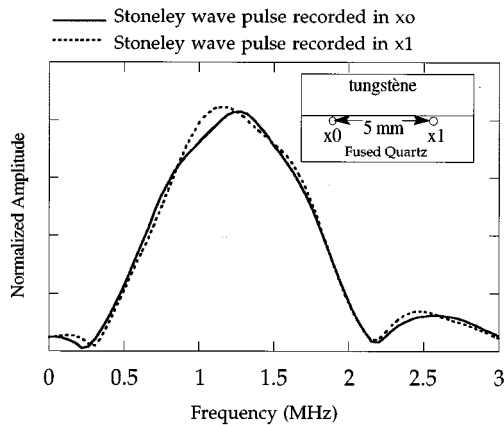


FIG. 7. Spectra of two time signals of a Stoneley wave at the tungsten–fused quartz interface recorded at the same depth and for two positions along the x_1 axes separated by 5 mm. No attenuation during the propagation is seen.

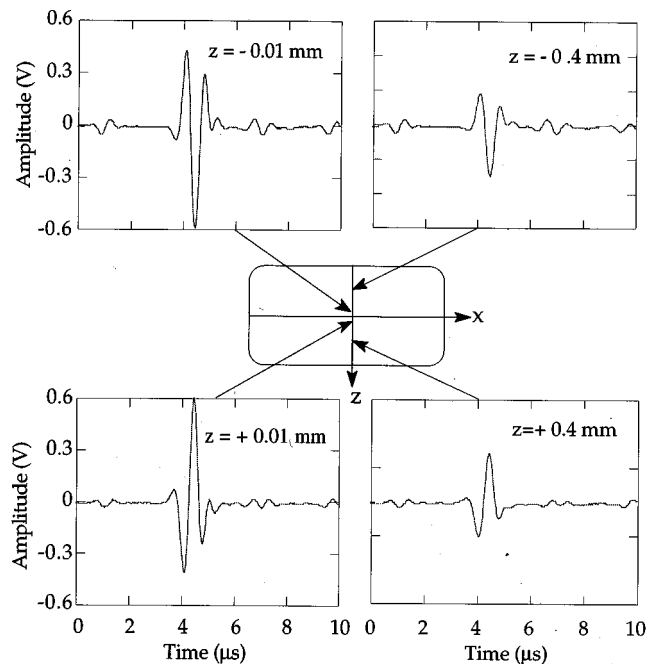


FIG. 8. Time signals corresponding to a scan in x_2 direction for the fused quartz–fused quartz slip interface.

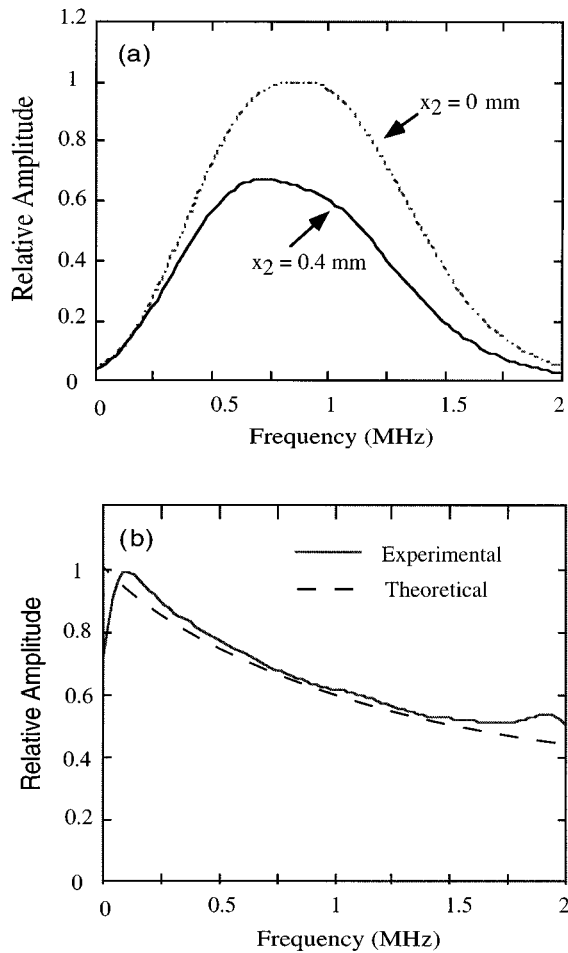


FIG. 9. Spectra of the time signals recorded for two different depths (a) and their ratio (b) showing the Stoneley wave decay in the x_2 direction as a function of frequency. The dashed line in (b) shows the calculated dilatational strain for the corresponding experimental conditions.

quency. The measurements are in good agreement with the predicted inhomogeneity of the Stoneley wave for this material combination.

B. Direct measurement of leaky interface wave

The case of a Plexiglas–fused quartz slip interface has been investigated. This combination of material supports do not support a Stoneley wave. If an interface wave propagates, it should be either an interface wave or a Rayleigh wave as described previously. As a matter of fact, a numerical investigation of the characteristic equation shows the existence of two complex roots corresponding to interface waves which can be excited:

$$\begin{aligned} k_x &= (1.079 + i0.086)k_{t_{\text{fused quartz}}}, \\ k_x &= (1.350 + i0.003)k_{t_{\text{fused quartz}}}, \end{aligned} \quad (9)$$

where $k_{t_{\text{fused quartz}}}$ is the shear wave number inside fused quartz. This material combination supports the simultaneous propagation of a Rayleigh wave [first root in (9)] and an interface wave and the aim of this part is to illustrate this special situation and to characterize the physical difference

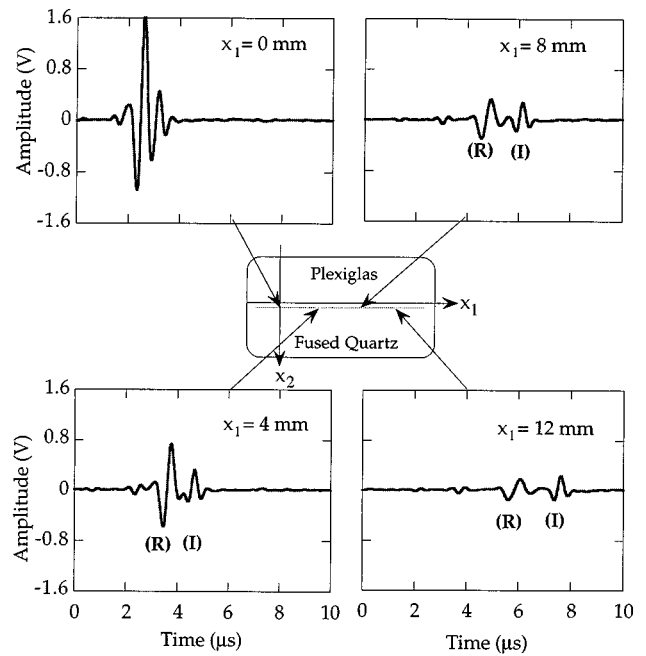


FIG. 10. Time signals corresponding to a scan in the x direction for the Plexiglas–fused quartz slip interface. The Rayleigh wave (R) and the interface wave (I) are clearly seen.

between these two modes using the interferometric detection method.

Figure 10 shows three time signals corresponding to a scan in the direction of propagation taken in the lower medium, i.e., fused quartz. The first signal is taken just after the conversion of the initial Rayleigh wave. Then during the propagation, two modes propagating with different velocities are clearly seen. In addition, these two modes propagate with different losses.

In order to characterize these two modes, the comparison between their velocities, attenuations, and field confinement at the interface is achieved. The measured velocities are 3.50×10^3 m/s for the faster mode and 2.70×10^3 m/s for the slower mode. The first mode propagates with a velocity close to the Rayleigh velocity in fused quartz (3.36×10^3 m/s), the second propagates with a velocity close to the longitudinal velocity in Plexiglas (2.68×10^3 m/s). These velocities are close to the ones deduced from the real part of the two solutions (9) which are 3.48×10^3 m/s and 2.71×10^3 m/s.

In order to measure attenuation along the direction of propagation, the principle of the procedure previously described for the inhomogeneity in the direction normal to the interface is applied, but the spectrum analysis is achieved for each pulse measured at constant x_2 and two different x_1 .

The corresponding losses for each modes are plotted as a function of the adimensional quantity $\Delta x/\lambda_{t_2}$, where λ_{t_2} is the shear wavelength in fused quartz (Fig. 11). They are also compared to the losses deduced from the imaginary parts of the two solutions (9). The attenuation due to the leakage into the Plexiglas is higher for the first mode so that the second mode is seen on a longer distance along the interface.

Finally, the amplitudes in the x_2 direction of these modes in each medium are determined from the experimen-

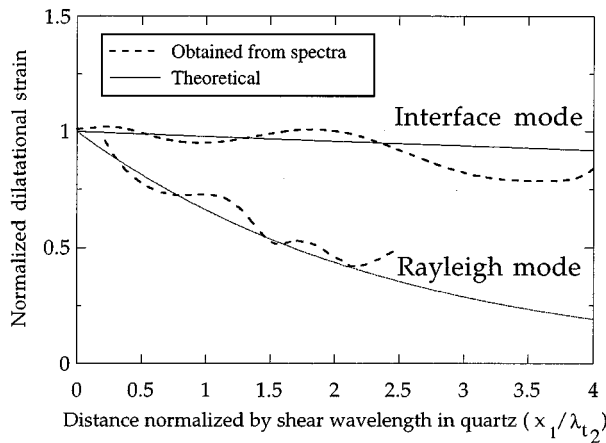


FIG. 11. Respective attenuation along the interface of each mode deduced from the spectra in function of distance normalized by the shear wavelength in fused quartz. The continuous lines are deduced from the imaginary parts of the wave vectors solutions of the characteristic equation.

tal data. They are represented in Fig. 12 for the first mode and in Fig. 13 for the second mode. The experimental data are compared to the theoretical inhomogeneities deduced from the calculation of the dilatation strain field. Both modes are confined inside fused quartz and the physical difference appears when considering the field inhomogeneities inside Plexiglas. The leakage of the first mode's longitudinal potential (proportional to the strain dilatation) is clearly seen: The amplitude in Plexiglas is higher with the distance to the interface. This mode corresponds with the solution called Rayleigh wave by Pilant. On the other hand, the second mode's longitudinal potential is slightly confined at the interface. This mode is analog to the solution called Interface wave by Pilant. The interface wave reradiates only in Plexiglas through the shear part of the potentials. Finally the dilatation strain measurements permit identification without ambiguity of the two solutions described by Pilant, the Rayleigh wave and the Interface wave, simultaneously detected for these material combinations.

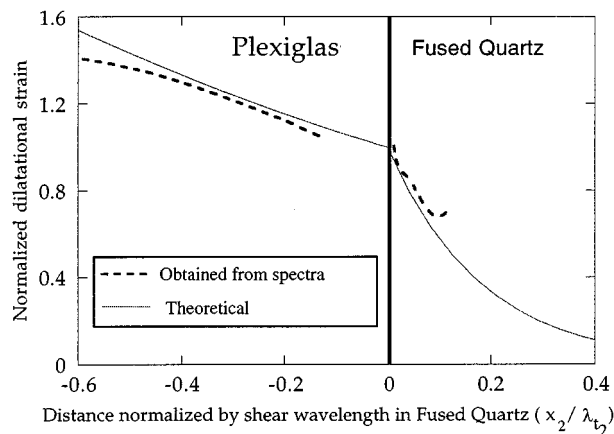


FIG. 12. Field amplitude deduced from the spectra in the direction perpendicular to the interface for the Rayleigh mode as a function normalized by the shear wavelength in fused quartz. The continuous lines are deduced from the wave vector solution of the characteristic equation.

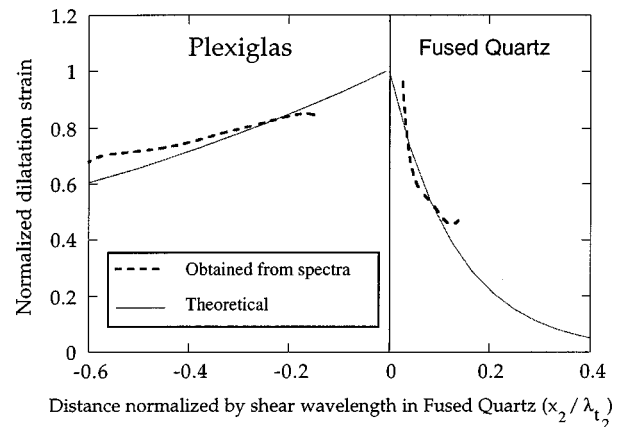


FIG. 13. Field amplitude deduced from the spectra in the direction perpendicular to the interface for the interface mode as a function normalized by the shear wavelength in fused quartz. The continuous lines are deduced from the wave vector solution of the characteristic equation.

IV. CONCLUSION

Direct measurements of several interface waves propagating along a solid–solid interface by optical means have been achieved. The detection technique, already used to detect Rayleigh and Lamb waves, is based on the interferometric detection of the optical phase shift of a laser beam induced by the crossing of an acoustical dilatation strain field inside a transparent medium. The classic case of a Stoneley wave propagating without loss along an interface has been illustrated. Velocity and confinement at the interface are determined from the scans in both normal and parallel directions to the interface. When the combination of materials does not support pure real celerity modes, one or two modes propagates with loss along the interface. These two modes exist simultaneously in the case of the combination fused quartz–Plexiglas. This situation has been experimentally illustrated. The features of the interferometric detection method have allowed a complete and straightforward characterization of these two modes. It gives access to more than just the velocities of the waves but also to their field inhomogeneities. These experimental results show the ability of this new optical detection method to characterize interface wave propagation because it leads to direct and quantitative measurements of the dilatational strain field inside transparent materials.

ACKNOWLEDGMENT

We want to thank Professor Laszlo Adler for a fruitful critical reading of this manuscript.

- ¹ *Research Techniques in Nondestructive Testing*, edited by R. S. Sharpe (Academic, New York, 1985).
- ² *Elastic Waves in the Earth*, edited by W. L. Pilant (Elsevier, New York, 1979).
- ³ L. J. Pirak-Nolte, L. R. Myer, and N. G. Cook, "Transmission of seismic waves across single natural fractures," *J. Geophys. Res.* **95**, 8617–8638 (1990).
- ⁴ S. I. Rokhlin and Y. J. Wang, "Analysis of boundary conditions for elastic wave interaction with an interface between two solids," *J. Acoust. Soc. Am.* **89**, 503–515 (1991).
- ⁵ R. Stoneley, "Elastic waves at the surface of separation of two solids," *Proc. R. Soc. London, Ser. A* **106**, 416–428 (1924).

- ⁶J. G. Sholte, "The range of existence of Rayleigh and Stoneley waves," *Mon. Not. R. Astron. Soc., Geophys. Suppl.* **5**, 120–126 (1947).
- ⁷G. S. Murty, "A theoretical model for the attenuation and dispersion of Stoneley waves at the loosely interface of elastic half-spaces," *Phys. Earth. Plan. Int.* **11**, 65–79 (1975).
- ⁸D. A. Lee and D. M. Corbly, "Use of interface waves for nondestructive inspection," *IEEE Trans. Sonics Ultrason.* **SU-24** (3), 206–212 (1977).
- ⁹R. O. Claus and C. H. Palmer, "Direct measurement of ultrasonic Stoneley wave," *Appl. Phys. Lett.* **31**, 547–548 (1977).
- ¹⁰C. B. Scruby and L. E. Drain, *Laser Ultrasonics* (Adam Hilger, New York, 1990).
- ¹¹X. Jia, Ch. Matteï, and G. Quentin, "Analysis of optical interferometric measurements of guided acoustic waves in transparent solid," *J. Appl. Phys.* **77**, 5528–5538 (1995).
- ¹²W. L. Pilant, "Complex roots of the Stoneley-wave equation," *Bull. Seismol. Soc. Am.* **62**, 285–299 (1972).
- ¹³Ch. Matteï, X. Jia, and G. Quentin, "Measurement of Rayleigh wave strains inside a transparent solid by optical interferometry," *Acustica united with Acta Acustica* **2**, 65–67 (1994).
- ¹⁴A. Korpel, *Acousto-optics* (Marcel Dekker, New York, 1988).
- ¹⁵A. Yariv and P. Yeh, *Optical Waves in Crystals* (Wiley, New York, 1984).
- ¹⁶D. Royer and E. Dieulesaint, "Optical detection of sub-ångström transient mechanical displacements," *Proc. IEEE Ultrason. Symp.* 527–529 (1986).
- ¹⁷B. Poirée and F. Luppé, "Evanescence plane waves and the Scholte-Stoneley interface wave," *J. Acoust.* **4**, 575–588 (1991).